Microsc. Microanal. 15, 20–29, 2009
doi:10.1017/S1431927609090023

Microscopy AND Microanalysis

Electron Diffraction Based Analysis of Phase Fractions and Texture in Nanocrystalline Thin Films, Part II: Implementation

János L. Lábár*

Research Institute for Technical Physics and Materials Science, H-1121 Budapest, Konkoly-Thege M. út 29-33, Hungary

Abstract: This series of articles describes a method that performs (semi)quantitative phase analysis for nanocrystalline transmission electron microscope samples from selected area electron diffraction (SAED) patterns. Volume fractions of phases and their textures are obtained separately in the method. First, the two-dimensional SAED pattern is converted into an X-ray diffraction–like one-dimensional distribution. Volume fractions of the nanocrystalline components are determined by fitting the spectral components, calculated for the previously identified phases with *a priori* known structures. Blackman correction is also applied to take into account dynamic effects for medium grain sizes. Peak shapes and experimental parameters (camera length, etc.) are refined during the fitting iterations. Parameter space is explored with the help of the Downhill-SIMPLEX algorithm. Part I presented the principles, while Part II now elaborates current implementation, and Part III will demonstrate its usage by examples. The method is implemented in a computer program that runs under the Windows operating system on IBM PC compatible machines.

Key words: electron diffraction, SAED, ring patterns, nanocrystals, thin films, phase fractions, texture, quantitative analysis, TEM

Introduction

The method, elaborated in this series of articles, is implemented in a form of a computer program, called "ProcessDiffraction." The first version of the program only contained qualitative phase analysis, i.e., identification of the crystalline phases that are the most probable components of the sample volume, analyzed by selected area electron diffraction (SAED) (Lábár, 2000). Extension of the dynamic range appeared separately (Lábár, 2002). Indexing of a (set of) SAED pattern(s) with ProcessDiffraction was published later (Lábár, 2005). Functionality of the program was significantly enhanced by the incorporation of quantitative phase analysis (the topic of the present series of articles); however, the name "ProcessDiffraction" was still retained.

Reading the principles in the first part of this series (Lábár, 2008) is absolutely necessary for the understanding of the implementation details, given in the present article.

Received January 15, 2008; accepted February 20, 2008
*E-mail: labar@mfa.kfki.hu

Program Functions and Implementations

The Project and Markers

The Project Concept

The "Project" contains all the input data together with all the performed processing steps and their results and the variables characterizing the given state of the program. When the project is saved, the operation can be interrupted and at a later moment it can be continued from the same point as if it had not been interrupted.

A special algorithm was developed to save and retrieve the project to ensure the maximum possible compatibility between different versions of the ProcessDiffraction program. The Project file is saved in simple text-file format in sections. Each section starts with the name of the section in squared brackets, like [Markers] and ends with the same name, the word "End" appended, like [Markers End]. Sections are loaded independently. If more data are in the section than anticipated, the rest of the section is skipped and loading continues in the next section. If less data are in the section than anticipated, the rest of variables are not loaded (remain empty) and the loading continues in the

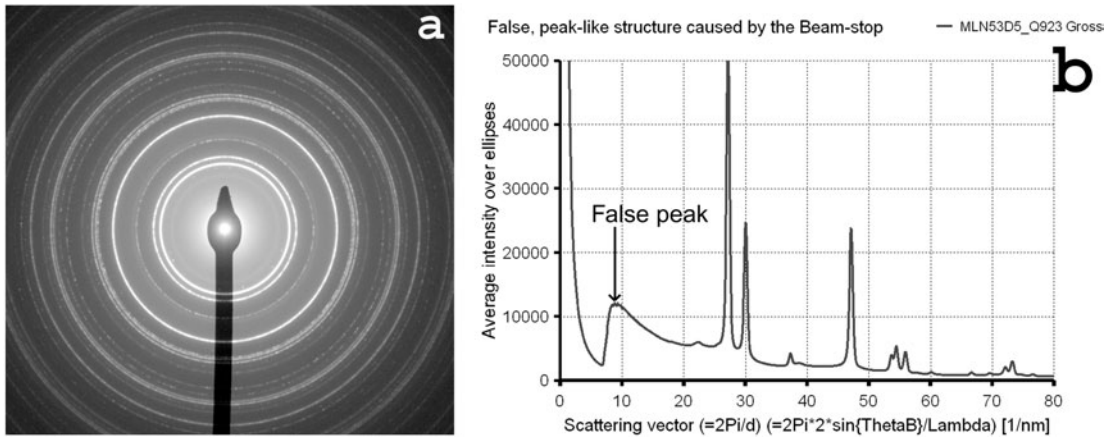

Figure 1. Intensity distribution with the distortion caused by the presence of the beam-stop in the original SAED pattern. **a:** The original pattern. **b:** The distribution calculated from it. The distortion resembles a broad peak at small scattering angles because low angle values are missing due to the presence of the beam-stop.

next section. That last situation may occur if the Project was saved with an older version. It is the operator's responsibility to give values for the not initialized data.

Because IP files might be as large as 64 Mbytes, and they may not be needed after the (much smaller) one-dimensional (1D) distribution was generated, there is an option to speed-load a project file without the original measured two-dimensional (2D) pattern. Resources as well as time and computer memory are saved by using this option. Obviously, if a later operation is also to be performed on the original 2D data, they must also be loaded.

The Marker Concept

A "Marker" in our method (and its implementation) means a set of diffraction *lines* (positions AND intensities, reflected in the height of the line). The set of lines together characterizes a crystalline phase with specific orientation distribution of grains. Randomly oriented and fully textured variants of the same phase will be described by separate Markers below.

During the quantitative fitting procedure, finite width and shape are also attached to each of the lines in a Marker and hence they are referred to as *peaks*.

Processing of Experimental Diffraction Patterns

Input Data

Digitally recorded[a] SAED patterns can be read into the program for processing from three different file formats. Beside the usual (uncompressed) bitmap (BMP) and tagged image file (TIF) formats, the proprietary file formats of imaging plates (IP) are also supported (both the IPL, IPH and IPC extensions). Compressed data formats are not supported in the present implementation.

Data can be either positive (large number corresponds to high intensity, as in a positive print, or in IP or in charge-coupled device (CCD) files) or, alternatively, they can be negative (e.g., for "scanned in" versions of photographic films). Nominal calibration values are supplied by the operator. Refinement of calibration data is discussed separately below.

The program also supports *merging* several patterns in order to extend the dynamic range of the data available in a single pattern. This option is useful if a wide range in scattering angles is to be examined and the dynamic range of the experimental data exceeds the dynamic range of the recording medium. Merging patterns, recorded with a series of exposure times, overcome that limitation in the dynamic range.

SAED Patterns and X-Ray Diffraction–Like Distributions

Measured SAED *patterns* are always 2D, as in Figure 1a. When the SAED pattern is averaged circularly, a 1D *distribution* (Fig. 1b) of diffracted intensities is obtained that resembles in appearance the conventional X-ray diffraction (XRD) powder patterns.

Derivation and Correction of the 1D Intensity Distribution

In contrast to the conventional X-ray power diffraction using X-ray counter, a SAED pattern is 2D. In an ideal ring pattern, the intensity would be uniform around a circle of a given radius. In a real pattern, the uniformity might not be perfect along a ring. In order not to lose information, the 2D pattern is circularly averaged to obtain an XRD-like, 1D distribution, where the intensity is plotted as a function of the length of the scattering vector. For the small scattering

[a]The program operates on previously saved SAED patterns and crystal structure information and also wants to save results, so the first thing to do is to specify for the program (in Options) where these data come from and where to store them.

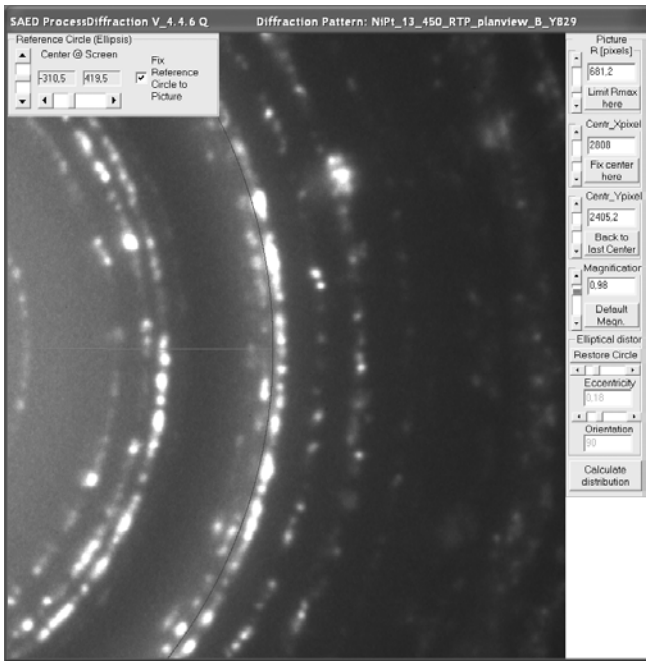

Figure 2. Part of the measured pattern with a section of the reference circle. The center of the pattern is off the screen.

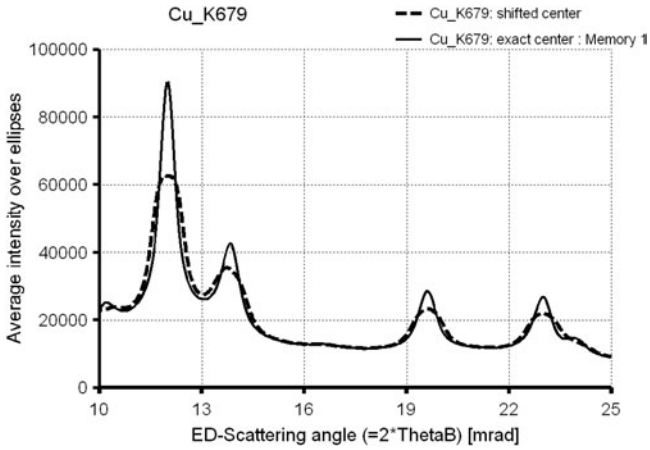

Figure 3. Comparison of the intensity distributions, calculated from a correctly centered and a slightly off-centered SAED pattern. Broadening of the peaks due to off-centering is seen. A broadening, very similar in appearance, is also caused by a small elliptical distortion, as discussed in text.

angles ($<5°$) encountered in SAED of high energy electrons, the length of the scattering vector is almost proportional to the scattering angle (only a minor correction is needed). Correction for a small elliptical distortion (due to the magnetic lenses) is done during this circular (elliptical) averaging, as described below.

Because the *center* of the diffraction pattern is determined by the direction of the straight-through (undeflected) beam that can be in an arbitrary position off from the geometrical center of the digital "image" (pattern), that center is located first. Centering is done in two steps. First, the rough position of the center is located manually, by generating a cross hair and a reference circle on the screen and moving the measured diffraction pattern relative to the reference circle until an experimental SAED ring coincides with the reference circle. For experimental situations, when the center of the pattern is off the recorded pattern, as in Figure 2, the reference circle can be moved, as an alternative to moving the pattern on the screen. As a next step, the rough center position is refined *automatically*. Rings in the 2D pattern, measured from polycrystalline (preferably nanocrystalline) patterns are assumed in that automatic procedure.[b] First, circularly averaged intensity is calculated as a function of the radius of the circles, using the current approximation for the location of the center. This 1D function shows peaks in the positions of the bright circles in the original 2D pattern. If the assumed center position is slightly off the true value, the peaks in the 1D distribution start to be smeared. The sharpest peaks with the highest peak-to-background (P/B) ratio will be obtained when the center is correctly positioned during the circular averaging. An example of a slightly off-centered and of a correctly centered pattern and the resulting distributions are shown in Figure 3. The automatic procedure locates the largest nonsaturated peak in the distribution, locates a relevant background position adjacent to this peak, and then tries to maximize the P/B ratio by slightly shifting the position of the assumed center around. In the course of center refinement, a larger step size is applied first, and then the search is repeated with finer (subpixel) step size around the position of the first maximum. The first, larger step size is adjusted to the automatically determined peak width.

Because the electromagnetic lenses in the transmission electron microscope (TEM) may cause slight distortions, an *elliptical distortion* is frequently present in the measured patterns. It means that the camera length (L) in one direction of the 2D patterns is slightly different from the L-value valid in a perpendicular direction. A similar distortion is also observed if the recording plane (of the film, IP or CCD) is not exactly perpendicular to the optical axis. That distortion (which is less than 2% for all the TEM SAED patterns encountered by the author) becomes obvious when a reference circle and the measured pattern are overlaid on the screen.[c] Correction for the elliptical distortion is also based on two steps. The first step is part of the previously de-

[b] A different approach is applied for spot patterns of single crystals, as described elsewhere (Lábár, 2005).

[c] The occasional screen distortion does not affect visual comparison because both the reference circle and the measured pattern are identically distorted by the screen, if any.

scribed manual centering. During that step, not only the center, but the eccentricity[d] and the direction of the reference ellipse are also adjusted, until visual agreement with the measured pattern is reached (Lábár, 2002). The following *automatic* procedure further refines the manually determined parameters of the ellipse. The procedure assumes that a well-separated ellipse (in the measured pattern) is selected by the overlaid reference ellipse on the screen. A belt is drawn around the reference ellipse, with user-specified width.[e] Points, with intensity above the background, are identified within this belt first. Then an ellipse is fitted with nonlinear least-squares method to the positions of the identified ring points.

Identification of the background intensity level is difficult, if a not too intense ring over a steeply varying background is selected as the basis of the parameter refinement, as shown in Figure 4. A weak ring in Figure 4a is marked by the reference circle. The same ring corresponds to the peak between $Q = 70$–90 in Figure 4b and shown in Figure 4c with linearly interpolated background. Threshold values are set from the interpolated background in the 1D distribution and used in the 2D pattern to identify individual bright spots, forming the points of the bright ring. Distances of the identified points from the pattern center are calculated and stored as a function of their angular position related to the horizontal x-axis on screen. The average distance of the identified points within 1° angular interval is calculated for each identified point. For an undistorted circle (with accurately known center), these distances are identical within statistical scatter (resulting in a constant distance as a function of angle). For an ellipse, a maximal value and a minimal value will be situated about 90° from each other. Ellipse parameters are determined from this angular distribution. The procedure performs the fitting in sections, so it can handle missing sections in the angular distribution,[f] as the one in Figure 5a. When a narrow missing section is detected, the distance values within it are calculated by interpolation from its two sides. Example of processing the pattern in Figure 1a is shown in Figure 5. When absolute minima and maxima in the distance versus angle curve are detected, a second-order polynomial is fitted to 30 points around it. The better approximations of the positions of the extremes are given by the apexes of these parabolas.

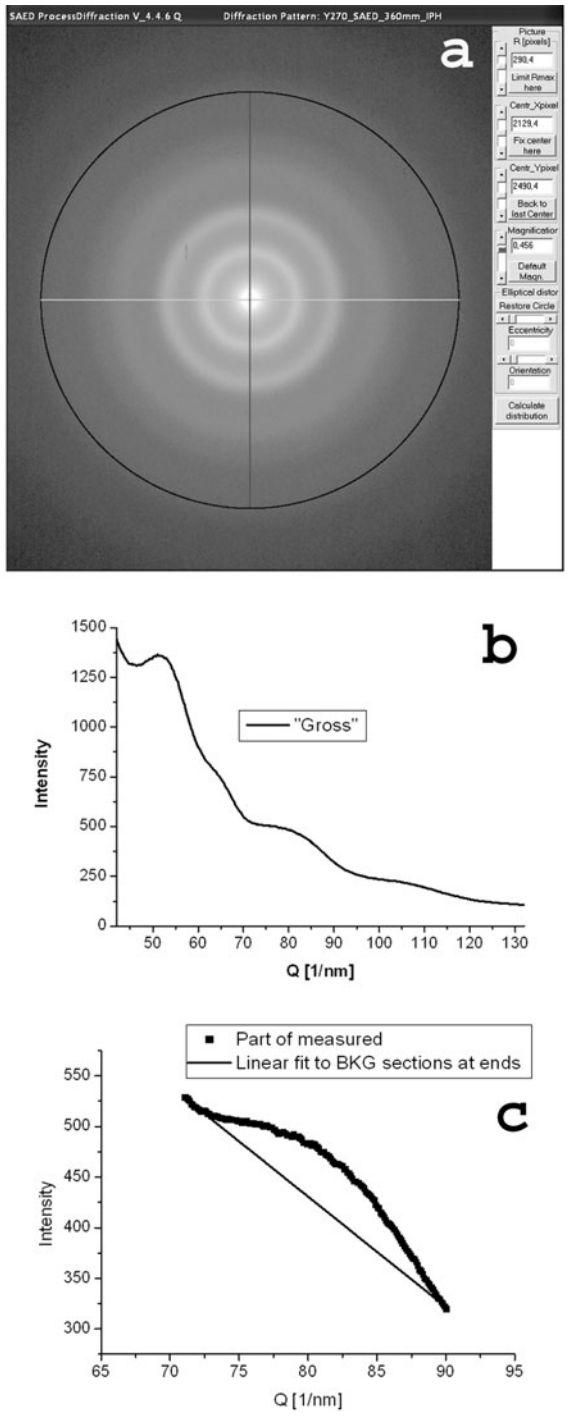

Figure 4. Problems of separating "background" from "over-the-background points," when a weak ring is superposed on a steeply varying background in the 2D pattern. A small peak is superposed on a steeply varying background in the corresponding 1D distribution. The apex of the peak may correspond to an intensity value, lower than the background at the left extreme (lowest angle) of the examined interval. Consequently, peaks cannot be located simply by finding the maximum in the given angular range. **a:** Measured 2D pattern. **b:** Part of the derived 1D distribution. **c:** Intensity distribution with indication of the background, interpolated for the selected ring from the extremes of the interval. It is obvious that the apex of the peak is not the maximum of the distribution.

[d]A correction in definition of quantities is also performed here. In early versions, the notion "eccentricity" was used incorrectly: in contrast to the name, the ratio of the long axis length to the short axis length was used in reality by the early program. From Version 4, the true linear eccentricity (e), in accordance with Math-book definition, is used ($e = c/a$, where c is the distance of the focus from the center and a is the large axis).

[e]Belt width must be selected to ensure that both sides of the belt correspond to background at the "feet" of the ring.

[f]Part of the ring might be missing from the experimental pattern when part of the pattern is blocked by a beam-stop or covered by a numbering unit of the microscope, or it might be missing if the center of the pattern is shifted off the measured pattern to protect the CCD.

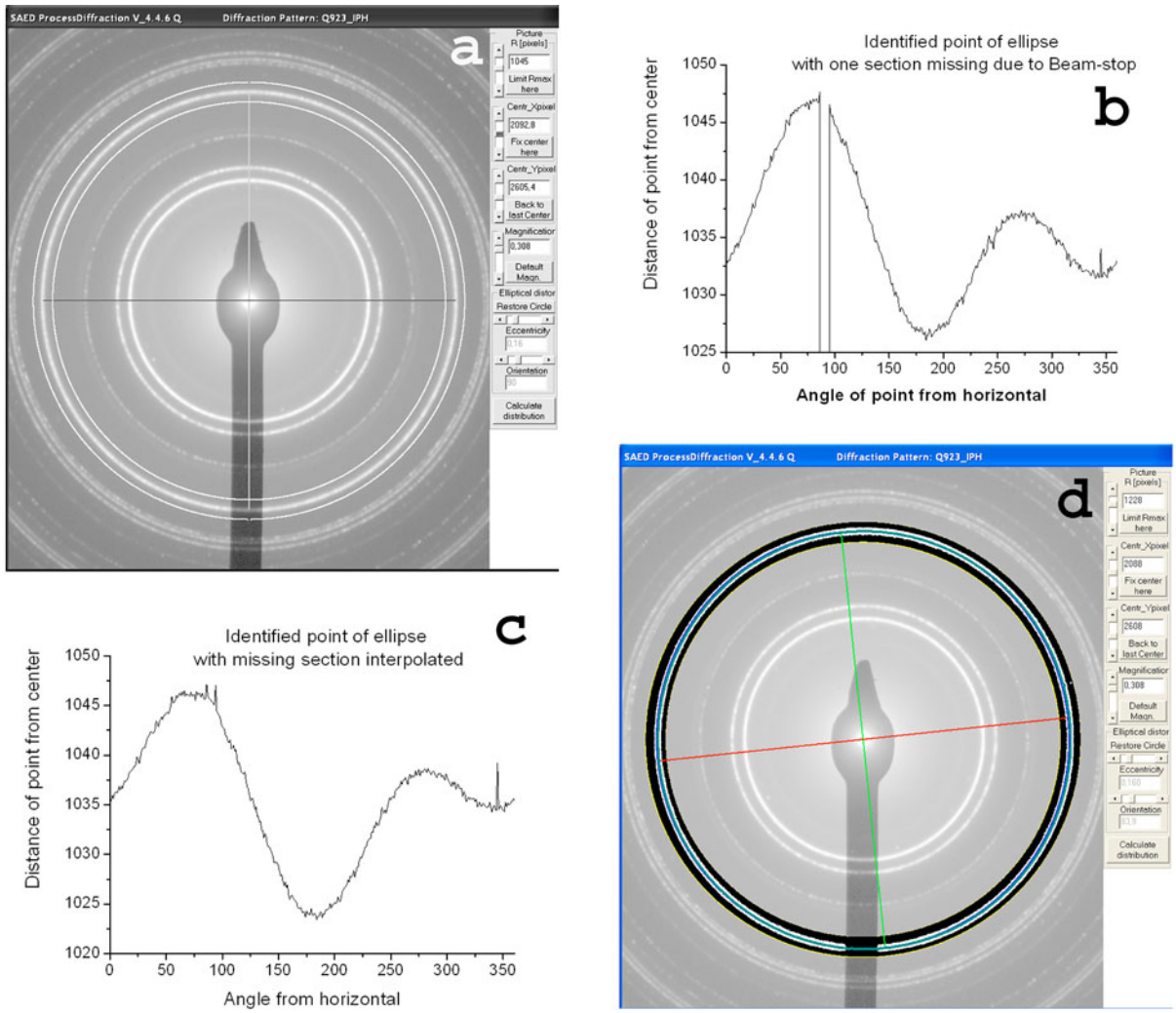

Figure 5. Average distance as a function of the angle between the horizontal and the vector pointing to the identified points. **a:** Part of the original patterns with indication of the belt. **b:** The missing section corresponds to the vertical belt, covered by the partially exposed beam-stop. **c:** The missing section is interpolated from its two sides. **d:** The identified points, used for fitting and the fitted ellipse, with the ellipse parameters indicated in the text boxes.

Because the effects caused by an incorrectly assumed position of the center and of an elliptical distortion are interdependent and appear similarly (as in Fig. 3), the refinement of the center on fine scale is also repeated here.

When both the center position and the elliptical distortion are calibrated, an average radius is ordered to the ellipse (the radius of the equivalent circle). Because the distortions are small,[g] the deviation between differently calculated equivalent radiuses is of the order of 10^{-5}. Geometric mean is used in the current implementation of the method.

[g]The distortion is <2%, i.e., $0.98 < b/a \leq 1$, where b and a are the small and large axes of the ellipse, respectively.

Calibration of Patterns

Nominal values for calibration of the measured patterns can be specified in three alternative ways. First, the camera constant and pixel size can be specified. Alternative way of specifying the same quantities is giving the accelerating voltage of the microscope and the camera length on the one hand and the resolution of the scanner (if negative films were digitized) on the other hand. The third alternative is to specify a single calibration value in 1/nm/pixel unit.

Calibration values can be refined in two steps. First, a Marker is overlaid the measured distribution and the user must double-click on a measured peak and also double-click on the Marker line that is known to correspond to the selected peak.

More accurate calibration is performed during parameter optimization of the quantitative phase analysis, as described below.

Units can be selected for the abscissa by double-clicking on any of the axes. The three possibilities are pixels (the least usual selection, because it does not carry any physical meaning), length of the scattering vector ($Q = 2\pi/d$) in 1/nm units, or scattering angle in milliradian units. The later two can only be activated after the pattern was calibrated.

Obviously, Markers can only be shown after the pattern was calibrated. Consequently, calibration is a required first step, before quantitative phase analysis can be started. The so-called "compare memories" are also activated only after calibration of the pattern.

Qualitative Analysis

The Peak Detection Process

Peak detection encounters three problems. First, the process must work equally well for broad peaks and narrow peaks. Second, it must operate reliably at different noise levels. Third, the peaks are sitting on a background that is changing differently at different sections of the same intensity distribution. To address these problems, ProcessDiffraction applies a filter first, to reduce the background. Peaks are identified in the filtered distribution, as a next step. A top-hat-function filter is applied, similarly to its application in either energy dispersive spectrometry (EDS) (McCarthy & Schamber, 1981) or in electron energy loss spectroscopy (EELS) (Leapman, 1992) spectrum processing. The filter width in this method must be adjusted to the peak width. The automatically determined peak width is used as a default, with possibility of manual override by the user. Furthermore, the peaks are identified in the filtered distribution, since the filtered distribution also has the peaks at the same locations where the original distribution has them, while the peaks are slightly narrower in the filtered distribution (although they are slightly distorted; however, this distortion does not harm identification of peak positions). Transitions of its first derivative from positive to negative are identified. Measured values at those locations are compared to the statistical standard deviation, as a threshold. Multiplier of the threshold can also be manually changed to adjust sensitivity to noise and also to detection of small peaks.

Structure Definition

To reduce typing chores to the minimum and to improve efficiency and, furthermore, to reduce the possibility of mistakes, *specification of the structure* for the computer separates into specifying crystal system, space group, and content of the asymmetric unit (in contrast to asking for all the atomic coordinates within the unit cell, which in the worst case mounts to a 196-fold reduction in the amount of typed data). The rest of the atomic positions is deduced automatically, using the symmetry operations of the space group. The following *consistency checks* are also included automatically. First, the automatically computed site multiplicity of any atomic coordinate is compared to the separately specified Wyckoff multiplicity. Second, atoms closer than a prespecified value are listed as a warning to avoid unintentional filling the same site with multiple atoms. Because sites can also be filled with fractional occupancies, it is also checked that sum of occupancies for any given site should not exceed one (= 1.00). Number of sites and total number of atoms (also influenced by occupancies) are also listed both for the asymmetric unit and for the entire unit cell. Volume of unit cell, atomic number density, and mass of the unit cell are also automatically calculated.

Identification of the Crystalline Phases

A very common situation in analyzing SAED ring patterns that the list of possible crystalline phases is not known *a priori*; however, the composition of the analyzed volume is known from complementary analysis by either EDS or EELS. In such situations the usage of the XRD powder diffraction files (Pdf-2, previously called JCPDS cards) is extremely useful because it lists the known phases and the positions of their diffraction lines. Although the intensities in it are strictly valid for XRD only, they also give an estimate that lines should be strong with electron diffraction, too. The database itself is NOT part of our program package; however, legal users of the database can interface to the database from within ProcessDiffraction[h] and use the XRD data as visual Markers aiding phase identification. Interfacing and usage of the Pdf-2 database are described below. All crystalline phases have to be identified prior to the next step of phase analysis.

Interfacing and Usage of the Pdf-2 Database

Interfacing the Pdf-2 database[i] to ProcessDiffraction is very simple. First, the location (drive and path) of the database itself must be specified in Options. The same, or a different drive and path, must be allocated to the indices, to be created by ProcessDiffraction. These index files are to be used by ProcessDiffraction only and are different from the index files used by the native search program that comes together with the database itself. Next, the indices must be generated (by a manually invoked[j] routine) to complete the interfacing procedure between the program and the database. Although generation of the index files is time-consuming, it is to be performed only once, during the

[h] The latest edition of the Pdf-2 database the author tested is from 2003.
[i] Trademark of International Center for Diffraction Data.
[j] If the interfacing step was not performed by the user before an attempt is made to use the database, an automatic procedure tries to detect the problem and tries to generate the index files. However, there are more possibilities for an error in such an automatic attempt to recover, due to incorrectly preassigned drives and directories. The safe way is the manually invoked automatic installation (interfacing) procedure.

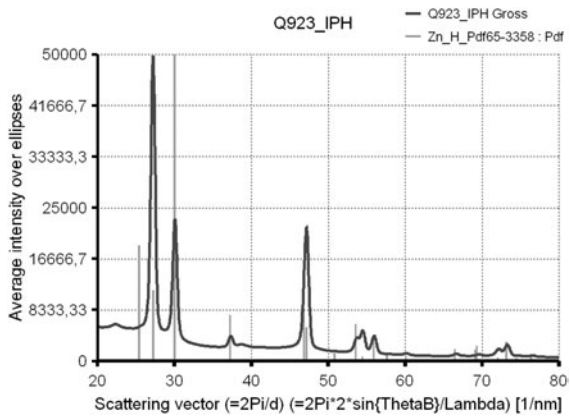

Figure 6. Appearance of a Marker (that was selected from the XRD database) as a set of lines overlaid the measured intensity distribution. In the example shown, all line positions (except one) seem to fit the measured peaks; however, the intensities are obviously deviating very much from the measured ones. Conclusion: either an incorrect phase was selected as a Marker or the possibility for the presence of a strong texture must be examined.

interfacing procedure. Index generation must NOT be interrupted. In case of incomplete index generation, the entire process must be repeated to prevent later faulty operation.

Application of the Pdf-2 database is helped by a graphical user interface (GUI). Phases can be selected on the basis of their component elements with several convenient filtering options. A single "card" of the database can also be retrieved immediately by its number. The selected phase(s) is/are shown visually overlaid to the measured distribution (Fig. 6).

A Simple Tool for Presentation of Qualitative Analysis Results

When the rings are identified, a labeled version of the measured pattern is frequently needed. ProcessDiffraction prepares such a labeled image automatically. Whenever a detected peak in the 1D distribution is within tolerance to a Marker line, the corresponding ring in the 2D pattern is labeled automatically with the name of that Marker line.

Graphical results (labeled patterns, distributions, Markers, fitted and measured distributions, etc.) can be inserted into a Document that can be saved as a rich text file. Results of quantitative analysis will also be inserted into that Document automatically (see below).

Quantification

Calculation of the Marker Data for Electron Diffraction

For qualitative phase identification, or for indexing of single crystal patterns, it is enough to know the positions of the diffracted lines, so XRD data from the power diffraction database can be used. However, to quantify the fraction of phases or of the textured component, the intensities of the diffracted electrons are also needed. Intensities of the diffracted electrons can only be calculated if the exact description of the crystal structure of the phases in question is available. Specification of the structure is performed within a larger crystallography package in ProcessDiffraction.

Calculation of Crystallographic Data

Another important aspect of the implemented crystallographic calculations is that they are placed on a unified platform. In contrast to using individual formulas for each crystal system to calculate spacings of the reflecting planes (d-values in the Bragg-equation) and angles between planes and/or between directions, furthermore calculating lengths of real-space and reciprocal space vectors, all of these calculations are carried out with the same formulas for all the crystal systems, using the *Metric matrix* and its inverse. These relations are also used in transforming real-space and reciprocal-space directions and in selecting planes (i.e., diffraction lines) that belong to a given zone (texture axis).

When *Markers* are calculated in ProcessDiffraction from the structure, automatic *enumeration* and sorting of diffraction lines between (-hmax, -kmax, -lmax) and (hmax, kmax, lmax) starts from zero, progressing in steps of ± 1 (symmetrically) in each index. This approach ensures that the lower index lines are included in the enumeration anyhow, even if some of the lines shall be skipped due to an overload in the number of lines. Reduction in the number of lines to be included in the Marker is done in two automatic *sorting* steps. First, lines are arranged by their d-values. Within a group that is characterized with a single d-value, lines with equivalent indices are listed first (on the basis of the symmetry of the crystal system), then the rest of the lines with the same d-value is grouped into other equivalence groups again (in case of accidental coincidence of d-values for nonequivalent lines, like 034 and 005 in the cubic system). Within an equivalence group, a representative index and the multiplicity is determined and stuck to a single member of the line group, the rest of the equivalence group members is deleted. This consolidated sorting of the lines makes the transition from single crystal diffraction 2D patterns (or better to say from 3D reciprocal space) to powder diffraction 1D distributions.

Dynamic Correction; Grain Size

Because the Blackman correction includes the size of the coherently scattering domain in the direction of the beam, that grain-size parameter can also be refined automatically from the fit. The dependence of line intensity on grain size is different for the different lines (see Part I, Lábár, 2008), so independent grain-size parameters can be determined for each phase (structure) from the condition that all relative line intensities must fit to the measured distribution simultaneously.

Textured Powder Patterns

Quantitative analysis must always be preceded by full qualitative analysis. The first step of quantification is that all Markers, corresponding to the phases, identified in the qualitative step must be generated "On the fly." The simplest case is when all phases are randomly oriented nanopowders. In that case one Marker per phase is needed. In case of partial fiber texture, two Markers are to be calculated for the textured phase—one for random orientation distribution and one for a fully textured version.

Presence of texture must always be tested by a tilting experiment when the patterns are recorded. Comparison of the measured distribution with the overlaid Marker(s) might give a hint if a significant fraction of a given phase may be in textured form or not. As a means of quantification, texture index can be calculated for each line, comparing experimental peak intensities from peak decomposition to calculated ones, calculated for random orientation distribution. If a low index line is very strongly underrepresented in the experimental pattern (as compared to the random Marker), a textured Marker is also to be generated, with texture axis not lying in the underrepresented planes.[k] Partial texture appears in the result as a significant volume fraction of the fully textured phase. Disregarding texture, which in fact is present in the measured distribution, may completely destroy the result, so selection of textured Markers is vital if texture is identified in the experimental distribution. (See the Results section in the upcoming Part III.) Be aware of the fact that not all textured patterns can be processed by the present implementation of our program (see Part I, Lábár, 2008).

A missing line does not fully characterize a texture. It is the responsibility of the operator to select a texture axis that is meaningful for the given system. The computer will never notice if we force it to fit meaningless Markers.

How Many Markers to Include?

As with all least-square fitting methods, good fit can only be expected if all independent model functions that contribute to the fitting interval are included in the list of models (Markers). In other words, all measured peaks must be present in the models and all peaks of the models must be observed in the measured peaks. If a peak of a model (Marker) is missing from the measured, see the procedure for texture. If a measured peak is "disregarded" by not assigning a Marker to it, no good fit can be anticipated. The bigger the disregarded peak, the more invalid the numerical result must be.

It is not the number of Markers, but the number of parameters to fit that is important in testing the limits of the usability (see below).

Case of Linearly Interdependent Markers

As it was elaborated in Part I (Lábár, 2008), volume fractions are obtained by matrix inversion, solving a set of over determined equations. Matrix inversion always fails if all the models are not linearly independent (in the examined interval). It may happen by accident that the same Markers are specified twice. Although there is a small chance of this happening intentionally, it may happen unintentionally without noticing. One of the possibilities is if Markers are calculated from the same structure for random orientation and also for a texture, while the fitting interval is so narrow that all lines of the two "independent" Markers coincide within the interval. Another possibility is that we start from two structures with different names but that have the same crystal structure and their respective lattice parameters are within the experimental resolution of the method.[l] Whenever the Gauss-Jordan matrix inversion routine gives an error message, this possibility is to be examined first because most probably a problem of incorrect Marker selection is the cause and not a bug in the program.

Temperature Factors

Whenever a Debye-Waller (DW) factor is changed in a structure, the affected Markers are recalculated. That happens if any (or all) of the DW factors are refined during the iteration loop. Several combinations of DW factors may be selected for refinement. The suggested default selection is separate calculation of a DW factor for each element in each structure.

Shapes and Widths of the Measured Peaks

The *lines* in the Marker are only characterized by position and intensity. When shape is also attributed to them, we speak of *peaks*. The extremes of selectable three[m] peak shapes (Gaussian and Lorentzian) can roughly be identified by visual inspection of the experimental distribution. The observed peak shape can change significantly from one experimental distribution to the other. Generally the best result can be achieved by selecting the more general pseudo-Voigt shape with identical widths for both the Gaussian and the Lorentzian components and with refinable fraction of the Gaussian component. Usually a single, constant line width for all lines of the same structure (including both the random and the textured Markers calculated from that

[k] Remember that planes are only seen in SAED, which lie in the zone that practically coincides with the viewing direction, due to the small Bragg angles, valid for high energy electron diffraction.

[l] For example, two face-centered cubic elements with lattice parameters may be very close to each other, so that the corresponding peaks of the two phases are within one pixel in the fitting interval.

[m] More shape options are to be included in future versions of the program.

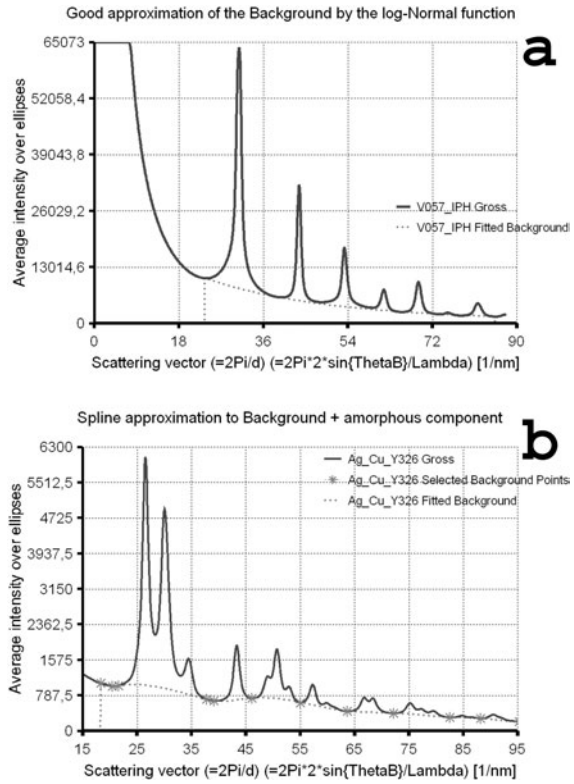

Figure 7. Measured intensity distribution, with background, fitted to the set of manually selected points. **a:** Lognormal model function, good for a sample containing NO amorphous component. **b:** Cubic-Spline model function, to include the effect of amorphous component into the background empirically. The selected points are indicated with asterisks.

same structure) provides good results. Although a possible linear dependence of the peak width with scattering vector is also incorporated, the author found that a constant peak width seems to be a good approximation for the distributions encountered up to now. The possible reason might be twofold. First, dislocations are not present with considerable density in nanocrystals. Second, in contrast to XRD, the intensity is recorded over a narrow angular range without a moving analyzer crystal.

Background under the Peaks; Effect of Amorphous Components

When a self-supporting thin film of polycrystalline material is examined and no amorphous component is present, the shape of the background is generally well approximated with a lognormal distribution function over a wide range of scattering vector lengths (Fig. 7a). However, when the layer is spread over a thin amorphous supporting film (e.g., amorphous carbon), total background, from the point of view of the peaks, includes both the "true" background and the broad diffuse peaks, originating from the presence of the amorphous component within the sampled volume. That effect is treated empirically in the current implementation, similarly as it is treated empirically in XRD (where a polynomial is fitted to the measured XRD distribution). A cubic-Spline function is fitted to the observed background in our method to tackle that problem. The undulations, caused by the amorphous peaks, can be followed empirically by marking enough points for background fitting and interpolating the background in between them by the cubic-Spline function (Press et al., 2007). The functions for Spline fitting in Numerical Recipes are translated from FORTRAN to Visual Basic to be used in our implementation. Figure 7b illustrates the shape of the empirical background for such a sample (the manually marked points are indicated by asterisks). The details of the interpolated background shape can be easily changed by varying the number and positions of the marked points. Although it is also provided as an option, the polynomial shape, which proved to be satisfactory in XRD, is generally not a good description of the shape of the background in SAED.

Parameter Optimization; Peak Decomposition versus Phase Analysis

Because there are many parameters that can be refined during the fitting procedure, they were divided into groups in the GUI to make the selection process clear-cut. The two main modes of operation for quantifying a powder pattern are peak decomposition and phase analysis. Peak decomposition simply means that we treat every peak as an independent entity and try to extract their integral intensities from the measured distribution, while their positions are fixed. Other parameters, like peak shapes and peak widths, are "by-products" of that procedure. It can be used to calculate texture indices. The other mode is phase analysis (our main subject in this article), which also may include refinement of some structure parameters. In phase analysis, the parameters of the peaks belonging to the same phase are constrained together. The intensity ratios are kept at the values that were calculated in the Markers.

It is important that parameter optimization should start as close to the global minimum as is possible. It can be ensured stepwise. First, rough, manual calibration should be performed in order that peaks will be searched close to their true values. The number of parameters must be restricted first and can only be increased step-by-step. A good start is to force all peaks to have the same shape at the beginning and allow different peak widths and peak shapes for the different phases as a next step. Start with random orientation distribution only and introduce textured forms in a later step. Start with kinematic approximation and allow dynamic correction together with refinement of grain size next. Start with a common grain size for all and allow different grain sizes later.

When a distribution in about 1,000 channels is fitted, fitting a maximum of 20 parameters seems to work reasonably well. These parameters can be: 1 camera length (or, as

an alternative, 1 lattice parameter for previously well-calibrated distribution), 2 shape and width parameters per phase (for 4 phases = 8), 1 grain size per phase (= 4), 1 temperature factor per element. These maximum 20 parameters are "freed-up" stepwise, starting from 3 (1 camera length, 1 shape, and 1 width).

Availability of the Program

The implementation, described in the present article, is made available free of charge simultaneously with the appearance of this article. It can be downloaded at http://www.mfa.kfki.hu/~labar/ProcDif. Remarks on either problems or on requests for later development are welcome by the author.

Conclusions

With the method presented in Part I (Lábár, 2008), (semi)-quantitative phase analysis became possible by processing electron diffraction patterns, recorded from nanocrystalline thin films in the TEM. The method is implemented in the form of a computer program that is written in Visual Basic and runs under the Windows operating system[n] on IBM PC compatible machines. Details of this implementation are given in the current article (Part II). Options of the present implementation can be user-friendly selected from different pages of the GUI. Details of the state of operation and all the results obtained up to a certain moment can be saved in a "Project" that can be later reloaded, and the operation can then be continued from the point where it was interrupted. Different, alternative data reduction routes can be tried and saved under different project names for comparison. For fiber-textured materials (which are very frequently present in thin films), the SAED pattern must be recorded from the direction of the texture axis to obtain full rings with homogeneous distribution of intensities along the rings. Volume fractions of the different phases and volume fraction of textured grains of a given phase are determined for the nanocrystalline phases. Dynamic effects are approximated by the Blackman formula. The effect of the amorphous components is minimized by an empirical interpolation of the background under the peaks. Application examples of the program are presented in the upcoming Part III of this article.

[n]Windows XP operating systems were tested the most.

Acknowledgments

The author is indebted to Olga Geszti for her persistent help in testing the computer program and providing continuous feedback for improvement. This program would not have been finished without her valuable help. Financial support of the Hungarian National Agency for Science and Technology is acknowledged (NKFP07-A2-METANANO).

References

Lábár, J.L. (2000). ProcessDiffraction: A computer program to process electron diffraction patterns from polycrystalline or amorphous samples. *Proc. EUREM 12*, Brno, Czech Republic, July 9–14, 2000, Ciampor, Frank L. & Ciampor, L. (Eds.), Vol. III, pp. I379–I380.

Lábár, J.L. (2002). A tool to help phase identification from electron diffraction powder patterns. *Microsc Anal* **75**, 9–11.

Lábár, J.L. (2005). Consistent indexing of a (set of) SAED pattern(s) with the ProcessDiffraction program. *Ultramicroscopy* **103**, 237–249.

Lábár, J.L. (2008). Electron diffraction based analysis of phase fractions and texture in nanocrystalline thin films; Part I: Principles. *Microsc Microanal* **14**(4), 287–295.

Leapman, R. (1992). EELS quantitative analysis. In *Transmission Electron Energy Loss Spectrometry in Materials Science*, Disko, M.M., Ahn, C.C. & Fultz, B. (Eds.), pp. 47–83. Warrendale, PA: TMS.

McCarthy, J.J. & Schamber, F.H. (1981). Least-squares fit with digital filter: A status report. In *Energy Dispersive X-Ray Spectrometry*, NBS Special Publications 604, Heinrich, K.F.J., Newbury, D.E., Myklebust, R.L. & Fiori, C.E. (Eds.). Malcolm Bridge: U.S. Department of Commerce.

Press, W.H., Teukolsky, S.A., Vetterling, W.T. & Flannery, B.P. (2007). *Numerical Recipes 3rd Edition: The Art of Scientific Computing*. Cambridge: Cambridge University Press.